

Synthesis of Zirconium, Hafnium, and Tantalum Complexes with Sterically Demanding Hydrazide Ligands

Jean-Sébastien M. Lehn, Saba Javed, and David M. Hoffman*

Department of Chemistry and the Center for Materials Chemistry, University of Houston, Houston, Texas 77204-5003

Received August 7, 2006

The bulky hydrazine $t\text{-BuN(H)NMe}_2$ was synthesized via hydrazone and $t\text{-BuN(H)N(H)Me}$ intermediates as the major component in a 90:5:5 mixture consisting of $t\text{-BuN(H)NMe}_2$, $t\text{-BuN(Me)N(H)Me}$, and $t\text{-BuN(Me)NMe}_2$. Reacting the mixture with $n\text{-BuLi}$ followed by distillation and fractional crystallization led to the isolation of the ligand precursor $\text{LiN}(t\text{-Bu})\text{NMe}_2$. Lithium hydrazides, LiN(R)NMe_2 , were reacted with metal chlorides to afford the hydrazide complexes $\text{M}(\text{N}(\text{Et})\text{NMe}_2)_4$ ($\text{M} = \text{Zr}$ or Hf), $\text{MCl}(\text{N}(\text{R})\text{NMe}_2)_3$ ($\text{M} = \text{Zr}$, $\text{R} = i\text{-Pr}$ or $t\text{-Bu}$; $\text{M} = \text{Hf}$, $\text{R} = t\text{-Bu}$), and $\text{TaCl}_3(\text{N}(i\text{-Pr})\text{NMe}_2)_2$. The X-ray crystal structures of $[\text{LiN}(i\text{-Pr})\text{NMe}_2]_4$, $[\text{LiN}(t\text{-Bu})\text{NMe}_2 \cdot \text{THF}]_2$, $\text{ZrCl}(\text{N}(\text{R})\text{NMe}_2)_3$ ($\text{R} = i\text{-Pr}$ or $t\text{-Bu}$), and $\text{TaCl}_3(\text{N}(i\text{-Pr})\text{NMe}_2)_2$ were determined. The structural analyses revealed that the hydrazide ligands in $\text{ZrCl}(\text{N}(\text{R})\text{NMe}_2)_3$ ($\text{R} = i\text{-Pr}$ or $t\text{-Bu}$) and $\text{TaCl}_3(\text{N}(i\text{-Pr})\text{NMe}_2)_2$ are η^2 coordinated.

Introduction

We described recently the synthesis of the trimethylhydrazido complexes $\text{M}(\text{N}(\text{Me})\text{NMe}_2)_4$ ($\text{M} = \text{Ti}$, Zr , or Hf) and $\text{TiCl}(\text{N}(\text{Me})\text{NMe}_2)_3$ ¹ and reported subsequently that, in combination with oxygen, the zirconium and hafnium derivatives were viable chemical vapor deposition precursors to the respective metal oxide films.² Prior to our synthetic work, $\text{Ge}(\text{N}(\text{Me})\text{NMe}_2)_4$ was the only structurally characterized homoleptic trialkylhydrazide complex reported.³ Halide–trimethylhydrazide derivatives were known and included $\text{SiCl}_2(\text{N}(\text{Me})\text{NMe}_2)_2$, $\text{TaCl}_3(\text{N}(\text{Me})\text{NMe}_2)_2$, and $\text{TiCl}_2(\text{N}(\text{Me})\text{NMe}_2)_2$.^{3–6} Other reported hydrazide complexes include $\text{Zn}(\text{N}(\text{H})\text{NH}_2)_2$,⁷ $\text{Be}(\text{N}(\text{R})\text{NH}_2)_2$ ($\text{R} = \text{H}$ or Me), $\text{EtBe}(\text{N}(\text{Me})\text{NH}_2)$, $[\text{EtBe}(\text{N}(\text{Me})\text{NMe}_2)]_n$, $[\text{EtBe}(\text{N}(\text{Me})\text{NHMe})]_n$, $[\text{EtBe}(\text{N}(\text{Me})\text{NH}_2)]_n$,⁸ $\text{Mg}(\text{N}(\text{Ph})\text{N}(\text{SiMe}_3)_2)_2$, $\text{Mg}(\text{N}(\text{SiMe}_3)\text{NMe}_2)_2$,⁹ $\text{M}(\text{N}(\text{SiMe}_3)\text{NMe}_2)_3$ ($\text{M} = \text{Ga}$ or In),¹⁰ $[\text{RZn}(\text{N}(\text{H})\text{NMe}_2)]_4$ ($\text{R} = \text{Me}$ or Et),¹¹ $[\text{EtZn}(\text{N}(\text{SiMe}_3)\text{NMe}_2)]_2$, $[\text{EtZn}(\text{N}(\text{Me})\text{NMe}_2)]_4$, $\text{Et}_4\text{Zn}_3(\text{N}(\text{Et})\text{NMe}_2)_2$, $[\text{EtZn}(\text{N}(i\text{-Pr})\text{NMe}_2)]_n$,¹² and several alkali metal derivatives having silyl and/or phenyl substituents.^{13–17} A extensive review on aluminum and gallium hydrazides has been published recently.¹⁸

Our successful preparation of metal oxide films from the $\text{M}(\text{N}(\text{Me})\text{NMe}_2)_4$ precursors prompted us to attempt the synthesis of other trialkylhydrazide complexes that might be used as film precursors. In this paper, we describe the syntheses of a new sterically encumbered hydrazide ligand precursor, $\text{LiN}(t\text{-Bu})\text{NMe}_2$, and the hydrazide complexes $\text{M}(\text{N}(\text{Et})\text{NMe}_2)_4$ ($\text{M} = \text{Zr}$ or Hf), $\text{MCl}(\text{N}(\text{R})\text{NMe}_2)_3$ ($\text{M} = \text{Zr}$, $\text{R} = i\text{-Pr}$ or $t\text{-Bu}$; $\text{M} = \text{Hf}$, $\text{R} = t\text{-Bu}$) and $\text{TaCl}_3(\text{N}(i\text{-Pr})\text{NMe}_2)_2$. As part of our studies, the X-ray crystal structures of $[\text{LiN}(i\text{-Pr})\text{NMe}_2]_4$, $[\text{LiN}(t\text{-Bu})\text{NMe}_2 \cdot \text{THF}]_2$, $\text{ZrCl}(\text{N}(\text{R})\text{NMe}_2)_3$ ($\text{R} = i\text{-Pr}$ or $t\text{-Bu}$), and $\text{TaCl}_3(\text{N}(i\text{-Pr})\text{NMe}_2)_2$ were determined.

Our successful preparation of metal oxide films from the $\text{M}(\text{N}(\text{Me})\text{NMe}_2)_4$ precursors prompted us to attempt the synthesis of other trialkylhydrazide complexes that might be used as film precursors. In this paper, we describe the syntheses of a new sterically encumbered hydrazide ligand precursor, $\text{LiN}(t\text{-Bu})\text{NMe}_2$, and the hydrazide complexes $\text{M}(\text{N}(\text{Et})\text{NMe}_2)_4$ ($\text{M} = \text{Zr}$ or Hf), $\text{MCl}(\text{N}(\text{R})\text{NMe}_2)_3$ ($\text{M} = \text{Zr}$, $\text{R} = i\text{-Pr}$ or $t\text{-Bu}$; $\text{M} = \text{Hf}$, $\text{R} = t\text{-Bu}$) and $\text{TaCl}_3(\text{N}(i\text{-Pr})\text{NMe}_2)_2$. As part of our studies, the X-ray crystal structures of $[\text{LiN}(i\text{-Pr})\text{NMe}_2]_4$, $[\text{LiN}(t\text{-Bu})\text{NMe}_2 \cdot \text{THF}]_2$, $\text{ZrCl}(\text{N}(\text{R})\text{NMe}_2)_3$ ($\text{R} = i\text{-Pr}$ or $t\text{-Bu}$), and $\text{TaCl}_3(\text{N}(i\text{-Pr})\text{NMe}_2)_2$ were determined.

* To whom correspondence should be addressed. E-mail: hoffman@uh.edu.

- (1) Lehn, J.-S. M.; Hoffman, D. M. *Inorg. Chim. Acta* **2003**, *345*, 327.
- (2) Lehn, J.-S. M.; Javed, S.; Hoffman, D. M. *Chem. Vap. Dep.* **2006**, *12*, 280.
- (3) Mitzel, N. W.; Smart, B. A.; Blake, A. J.; Parsons, S.; Rankin, D. W. H. *J. Chem. Soc. Dalton Trans.* **1996**, 2095.
- (4) O'Flaherty, F. P.; Henderson, R. A.; Hughes, D. L. *J. Chem. Soc. Dalton Trans.* **1990**, 1087.
- (5) Hughes, D. L.; Jimenez-Tenorio, M.; Leigh, G. J.; Walker, D. G. *J. Chem. Soc. Dalton Trans.* **1989**, 2389.
- (6) Scheper, J. T.; McKarns, P. J.; Lewkebandara, T. S.; Winter, C. H. *Mat. Sci. Semicond. Process.* **1999**, *2*, 149.
- (7) Goubeau, J.; Kull, U. *Z. Anorg. Allg. Chem.* **1962**, *316*, 182.
- (8) Fetter, N. R. *Can. J. Chem.* **1984**, *62*, 861.
- (9) Sachdev, H. *Eur. J. Inorg. Chem.* **2002**, 2681.

- (10) Luo, B.; Cramer, C. J.; Gladfelter, W. L. *Inorg. Chem.* **2003**, *42*, 3431.
- (11) Jana, S.; Fröhlich, R.; Mitzel, N. W. *Chem. Eur. J.* **2006**, *12*, 592.
- (12) Javed, S.; Hoffman, D. M. *Abstracts of Papers*, 62nd Southwest Regional Meeting of the American Chemical Society, Houston, TX; American Chemical Society: Washington, DC, 2006; 561.
- (13) Drost, C.; Jäger, C.; Freitag, S.; Klingebiel, U.; Noltemeyer, M.; Sheldrick, G. M. *Chem. Ber.* **1994**, *127*, 845.
- (14) Dielkus, S.; Drost, C.; Herbst-Irmer, R.; Klingebiel, U. *Angew. Chem., Int. Ed. Engl.* **1993**, *32*, 1625.
- (15) Gemünd, B.; Nöth, H.; Sachdev, H.; Schmidt, M. *Chem. Ber.* **1996**, *129*, 1335.
- (16) Metzler, N.; Nöth, H.; Sachdev, H. *Angew. Chem., Int. Ed. Engl.* **1994**, *33*, 1746.
- (17) Bode, K.; Klingebiel, U.; Noltemeyer, M.; Witte-Abel, H. *Z. Anorg. Allg. Chem.* **1995**, *621*, 500.
- (18) Uhl, W. *Struct. Bonding* **2003**, *105*, 42.

Experimental Section

General Procedures and Reagents. Solvents were purified following standard procedures and stored in the glove box over molecular sieves. The metal halides and *t*-BuN(H)NH₂·HCl were purchased from Strem Chemicals, Inc. and Sigma-Aldrich Corp., respectively, and used as received. The hydrazines EtN(H)NMe₂ and *i*-PrN(H)NMe₂ were prepared using modified literature procedures and dried by distillation over CaH₂.^{5,19,20} The modification to the established procedures involved carefully dropping concentrated aqueous solutions of the hydrazinium chloride salts obtained from the lithium aluminum hydride reductions onto hot NaOH pellets to afford the neutral hydrazines directly via distillation rather than neutralizing the salts, extracting with organic solvent, and then distilling from the extracts (e.g., see the synthetic procedure below for *t*-BuN(H)N(H)Me). Nuclear magnetic resonance spectra were recorded on a 300-MHz instrument and were referenced internally to the residual protons (¹H) or carbon atoms (¹³C) of the deuterated solvents. Infrared spectra were recorded on a Mattson Instruments FT-IR spectrometer. Midwest Microlab, Indianapolis, IN, performed the microanalysis.

LiN(*i*-Pr)NMe₂. A cold solution (−25 °C) of 1-*i*-propyl-2,2-dimethylhydrazine (10. g, 0.10 mol) in hexanes (100 mL) was added slowly to a cold solution (−25 °C) of *n*-butyllithium in hexanes (1.6 M, 60 mL, 0.096 mol, diluted with 100 mL of hexanes). When the addition was completed, the solution was allowed to warm to room temperature, whereupon it was stirred for an additional 12 h. The hexanes were then removed under vacuum. A minimum amount of hexanes (30 mL) was added to the residue, which dissolved completely. White crystals formed upon cooling (−25 °C) the solution (yield 5.7 g, 55%). ¹H NMR (C₆D₆): δ 3.56 (sept, 1, 6.6 Hz, (CH₃)₂NN(Li)(CH(CH₃)₂)), 2.49 (s, 6, (CH₃)₂NN(Li)(CH(CH₃)₂)), 1.21 (d, 6, 6.6 Hz, (CH₃)₂NN(Li)(CH(CH₃)₂)). ¹³C{¹H} NMR (C₆D₆): δ 48.0 (s, (CH₃)₂NN(Li)(CH(CH₃)₂)), 29.9 (s, (CH₃)₂NN(Li)(CH(CH₃)₂)), 26.7 (s, (CH₃)₂NN(Li)(CH(CH₃)₂)). IR (neat, NaCl, cm^{−1}): 2952 vs, 2854 vs, 2807 m, 2766 s, 2590 vw, 1530 m, 1447 vs, 1376 s, 1363 m, 1348 w, 1244 m, 1198 w, 1144 s, 1119 s, 1076 w, 1015 m, 985 w, 962 m, 894 s, 848 m, 777 w, 754 m.

***t*-BuN(H)N(H)Me.** *t*-Butylhydrazine hydrochloride (101 g, 0.812 mol) was dissolved in water (300 mL) under an argon atmosphere, and diethyl ether (300 mL) was added to the reaction flask. Sodium hydroxide (32.5 g, 0.812 mol) was added slowly in small increments over 2 h. After the NaOH was added and dissolved completely, formaldehyde (24.4 g, 0.812 mol) was added slowly to the reaction mixture. The mixture was stirred at room temperature for 6 h. The phases were then separated, and the organic phase was washed with distilled water (1 × 20 mL) and twice with a water solution saturated with NaCl (2 × 40 mL). The ether was removed by distillation. A small amount of hexanes (40 mL) was added to the liquid residue, and the solution was washed again with a water solution saturated with NaCl (2 × 40 mL). Most of the hexanes were then removed by distillation, yielding a solution of *t*-BuN(H)N=CH₂ in hexanes (79 mass % *t*-BuN(H)N=CH₂ by ¹H NMR analysis; yield 76.7 g, 95%). The hexanes solution of *t*-BuN(H)N=CH₂ was then added slowly to a cold solution (−25 °C) of LiAlH₄ (37.9 g, 1.00 mol) in diethyl ether (1200 mL) under nitrogen. The addition was stopped whenever the ether began to boil. After the addition was completed, the mixture was stirred for 12 h. An aliquot was removed periodically to determine by ¹H NMR analysis whether *t*-BuN(H)N=CH₂ remained in the solution. After no *t*-BuN-

(H)N=CH₂ remained, the flask was cooled (−18 °C) and small pieces of ice were added slowly to the cold mixture. The temperature of the solution was monitored, and if the temperature approached 20 °C, the addition was stopped until the mixture cooled again. After hydrogen gas evolution ceased, the mixture was allowed to warm to room temperature. A cold (0 °C) 5 M HCl solution (800–900 mL) was then added slowly to the mixture until the aluminum salts were completely dissolved. After the addition was completed, the pH was checked with litmus paper to verify that the medium was acidic. The two phases were separated, the organic phase was discarded, and the aqueous phase containing *t*-BuN(H)N(H)Me·HCl was washed with diethyl ether (1 × 30 mL). The aqueous solution was then reduced in volume (to ≈700 mL) by warming it (35 °C) under vacuum for 5 h. Sodium hydroxide pellets (800 g, 20.0 mol) were loaded in a two-neck flask equipped with an addition funnel and distillation head, and the flask was immersed in a hot (150 °C) oil bath for 1 h. The concentrated aqueous solution of *t*-BuN(H)N(H)Me·HCl was added rapidly via the addition funnel to the hot pellets of sodium hydroxide (**CAUTION: exothermic reaction**), and *t*-BuN(H)N(H)Me immediately began distilling into the receiving flask. The collected product, *t*-BuN(H)N(H)Me, was redistilled three times under argon, the first two distillations over NaOH pellets and the third over CaH₂ (yield 55.2 g, 67% based on *t*-BuN(H)NH₂·HCl). ¹H NMR (C₆D₆): δ 2.45 (br, 2, (CH₃)₃CN(H)N(H)(CH₃)), 2.37 (s, 3, (CH₃)₃CN(H)N(H)(CH₃)), 1.02 (s, 9, (CH₃)₃CN(H)N(H)(CH₃)). ¹³C{¹H} NMR (C₆D₆): δ 53.03 (s, (CH₃)₃CN(H)N(H)(CH₃)), 40.86 (s, (CH₃)₃CN(H)N(H)(CH₃)), 27.75 (s, (CH₃)₃CN(H)N(H)(CH₃)). IR (neat, NaCl, cm^{−1}): 3276 b, 2968 vs, 2866 m, 2781 m, 1606 w, 1477 s, 1446 s, 1383 s, 1360 vs, 1311 vw, 1232 vs, 1217 vs, 1130 w, 1111 w, 1036 vw, 1024 w, 982 vw, 918 s, 879 vs, 775 vw, 708 m. ¹H NMR of the intermediate *t*-BuN(H)N=CH₂ (C₆D₆): δ 6.13 (d, 1, 12.8 Hz, (H₃C)₃CN(H)N=CH₂), 5.91 (d, 1, 12.8 Hz, (H₃C)₃CN(H)N=CH₂), 4.63 (b, 1, (H₃C)₃CN(H)N=CH₂), 1.11 (s, 9, (H₃C)₃CN(H)N=CH₂). ¹³C{¹H} NMR (C₆D₆): δ 125.62 (s, (H₃C)₃CN(H)N=CH₂), 53.08 (s, (H₃C)₃CN(H)N=CH₂), 28.54 (s, (H₃C)₃CN(H)N=CH₂).

LiN(*t*-Bu)NMe₂. A cold solution (−25 °C) of *n*-butyl lithium in hexanes (1.6 M, 67.4 mL, 0.108 mol) was added slowly to a cold solution (−25 °C) of dry *t*-BuN(H)N(H)Me (11.0 g, 0.108 mol) in diethyl ether (300 mL). The solution was allowed to warm slowly to room temperature, whereupon it was stirred an additional 6 h. The solution was then cooled to −78 °C and a cold solution (−78 °C) of methyl iodide (15.3 g, 0.108 mol) in diethyl ether (35 mL) was added dropwise. After the addition was completed, the solution was allowed to warm slowly (12 h) to room temperature. Proton NMR analysis indicated the solution contained *t*-BuN(H)NMe₂ and minor amounts of unreacted *t*-BuN(H)N(H)Me and the side-products *t*-BuN(Me)N(H)Me, *t*-BuN(Me)NMe₂, and [*t*-BuN(R)NMe₃⁺][I[−]] (R = H or Me). A cold 1 M HCl solution (≈1.1 mol HCl) was added to the mixture, and the phases were separated. The aqueous phase was washed with ether (2 × 20 mL) and then placed under vacuum for 2 h to eliminate the remaining diethyl ether. The acidic solution was cooled (−5 °C) and then added to a flask containing a cold solution of 5 M sodium hydroxide (≈0.50 mol) and benzene (50 mL). The salts [*t*-BuN(R)NMe₃⁺][I[−]] (R = H or Me) precipitated, while the neutral hydrazines went into the benzene phase. The benzene solution was washed with 2 M NaOH (2 × 20 mL), which removed *t*-BuN(H)N(H)Me. The benzene solution was distilled over CaH₂ under argon, resulting in a benzene solution containing *t*-BuN(H)NMe₂, *t*-BuN(Me)N(H)Me, and *t*-BuN(Me)NMe₂ in an approximately 90:5:5 ratio (yield of *t*-BuN(H)NMe₂: ≈7.52 g, 60%) [¹H NMR (C₆D₆) of *t*-BuN(H)NMe₂: δ

(19) Klages, F.; Nober, G.; Kircher, F.; Bock, M. *Ann.* **1941**, 547, 1.

(20) Zinner, G.; Boehlke, H.; Kliegel, W. *Arch. Pharm.* **1966**, 299, 245.

2.28 (s, 6, $(\text{CH}_3)_3\text{CN}(\text{H})\text{N}(\text{CH}_3)_2$), 1.05 (s, 9, $(\text{CH}_3)_3\text{CN}(\text{H})\text{N}(\text{CH}_3)_2$); $^{13}\text{C}\{^1\text{H}\}$ NMR (C_6D_6): δ 53.82 (s, $(\text{CH}_3)_3\text{CN}(\text{H})\text{N}(\text{CH}_3)_2$), 50.95 (s, $(\text{CH}_3)_3\text{CN}(\text{H})\text{N}(\text{CH}_3)_2$), 28.36 (s, $(\text{CH}_3)_3\text{CN}(\text{H})\text{N}(\text{CH}_3)_2$).

The dry benzene solution of *t*-BuN(H)NMe₂, *t*-BuN(Me)NMe₂, and *t*-BuN(Me)N(H)Me was cooled (-20°C), and a cold solution of *n*-BuLi in hexanes (1.6 M, 44 mL, 0.070 mol) was added dropwise. After the addition was completed, the mixture was allowed to warm to room temperature, whereupon it was stirred for an additional 12 h. The benzene, hexanes, and unreacted *t*-BuN(Me)NMe₂ were removed under vacuum, leaving a mixture of LiN(*t*-Bu)NMe₂ and *t*-BuN(Me)N(Li)Me in an approximately 95:5 ratio. Two crystallizations from cold hexanes solutions (-25°C) produced LiN(*t*-Bu)NMe₂ as colorless crystals (yield 3.95 g, 30% based on *t*-BuN(H)N(H)Me). Anal. Calcd for $\text{C}_6\text{H}_{15}\text{LiN}_2$: C, 59.00; H, 12.38; N, 22.94. Found: C, 58.51; H, 12.17; N, 22.79. ^1H NMR (C_6D_6): δ 2.57 (s, 6, $(\text{CH}_3)_3\text{CN}(\text{Li})\text{N}(\text{CH}_3)_2$), 1.27 (s, 9, $(\text{CH}_3)_3\text{CN}(\text{Li})\text{N}(\text{CH}_3)_2$). $^{13}\text{C}\{^1\text{H}\}$ NMR (C_6D_6): δ 56.89 (s, $(\text{CH}_3)_3\text{CN}(\text{Li})\text{N}(\text{CH}_3)_2$), 52.34 (s, $(\text{CH}_3)_3\text{CN}(\text{Li})\text{N}(\text{CH}_3)_2$), 33.04 (s, $(\text{CH}_3)_3\text{CN}(\text{Li})\text{N}(\text{CH}_3)_2$). IR (neat, NaCl, cm^{-1}): 3072 w, 2960 s, 2939 vs, 2872 w, 2852 w, 2823 s, 2777 vs, 2729 vs, 2661 w, 1448 s, 1414 vw, 1375 s, 1348 s, 1232 w, 1213 m, 1192 s, 1142 s, 1078 m, 1022 w, 1005 s, 989 w, 910 vs, 833 s, 756 s.

Zr(N(Et)NMe₂)₄. Lithium 1-ethyl-2,2-dimethylhydrazide (0.578 g, 6.15 mmol) was added to a suspension of ZrCl₄ (0.350 g, 1.50 mmol) in diethyl ether (100 mL). The mixture was stirred at room temperature for 18 h before the ether was removed under vacuum to yield a yellow powder. Hexanes (40 mL) were added to the residue, and the mixture was filtered over Celite. The clear yellow filtrate was evaporated under vacuum, and the resulting yellow powder was sublimed twice ($120^\circ\text{C}/0.06$ mmHg). Zr(N(Et)NMe₂)₄ was collected as a light yellow waxy solid on the cold finger (yield 0.357 g, 54%). Anal. Calcd for $\text{C}_{16}\text{H}_{44}\text{N}_8\text{Zr}$: C, 43.70; H, 10.08; N, 25.48. Found: C, 43.72; H, 9.82; N, 25.32. ^1H NMR (C_6D_6): δ 3.29 (q, 8, 7.2 Hz, $\text{N}(\text{CH}_2\text{CH}_3)\text{N}(\text{CH}_3)_2$), 2.47 (s, 24, $\text{N}(\text{CH}_2\text{CH}_3)\text{N}(\text{CH}_3)_2$), 1.28 (t, 12, 7.2 Hz, $\text{N}(\text{CH}_2\text{CH}_3)\text{N}(\text{CH}_3)_2$). $^{13}\text{C}\{^1\text{H}\}$ NMR (C_6D_6): δ 45.80 (s, $\text{N}(\text{CH}_2\text{CH}_3)\text{N}(\text{CH}_3)_2$), 39.95 (s, $\text{N}(\text{CH}_2\text{CH}_3)\text{N}(\text{CH}_3)_2$), 18.14 (s, $\text{N}(\text{CH}_2\text{CH}_3)\text{N}(\text{CH}_3)_2$). IR (neat, NaCl, cm^{-1}): 3001 vw, 2935 vs, 2898 vw, 2850 vs, 2803 s, 2666 m, 2570 vw, 1524 vw, 1453 vs, 1385 w, 1368 w, 1337 m, 1246 vw, 1217 s, 1183 s, 1141 vs, 1118 s, 1062 s, 994 m, 963 m, 919 m, 865 m, 793 s, 736 m.

Hf(N(Et)NMe₂)₄. This compound, a waxy yellow solid, was prepared by using the method described for Zr(N(Et)NMe₂)₄. It was purified by sublimation, producing a waxy yellow solid on the cold finger (yield 57%). ^1H NMR (C_6D_6): δ 3.35 (q, 8, 7.2 Hz, $\text{N}(\text{CH}_2\text{CH}_3)\text{N}(\text{CH}_3)_2$), 2.49 (s, 24, $\text{N}(\text{CH}_2\text{CH}_3)\text{N}(\text{CH}_3)_2$), 1.28 (t, 12, 7.2 Hz, $\text{N}(\text{CH}_2\text{CH}_3)\text{N}(\text{CH}_3)_2$). $^{13}\text{C}\{^1\text{H}\}$ NMR (C_6D_6): δ 45.80 (s, $\text{N}(\text{CH}_2\text{CH}_3)\text{N}(\text{CH}_3)_2$), 40.19 (s, $\text{N}(\text{CH}_2\text{CH}_3)\text{N}(\text{CH}_3)_2$), 18.23 (s, $\text{N}(\text{CH}_2\text{CH}_3)\text{N}(\text{CH}_3)_2$). IR (neat, KBr, cm^{-1}): 2960 vs, 2940 vs, 2852 vs, 2805 vs, 2669 vs, 2573 vs, 2393 s, 2260 m, 2171 m, 2113 w, 1986 w, 1944 w, 1903 vw, 1845 vw, 1751 w, 1714 w, 1599 vs, 1454 vs, 1412 vw, 1385 w, 1369 w, 1340 m, 1298 m, 1250 w, 1219 s, 1190 s, 1144 s, 1123 w, 1062 s, 995 s, 957 m, 922 m, 874 s, 812 w, 793 vs, 735 vs.

ZrCl(N(*i*-Pr)NMe₂)₃. Lithium 1-*i*-propyl-2,2-dimethylhydrazide (0.324 g, 3.00 mmol) was added to a suspension of ZrCl₄ (0.233 g, 1.00 mmol) in cold (-25°C) diethyl ether (100 mL). The mixture was stirred at room temperature for 18 h before the ether was removed under vacuum to yield a yellow powder. Hexanes (40 mL) were added to the residue, and the mixture was filtered over Celite. The clear yellow filtrate was evaporated under vacuum, yielding a light yellow powder that was pure by ^1H NMR analysis (yield 0.382 g, 89%). If desired, ZrCl(N(*i*-Pr)NMe₂)₃ can be sublimed under

reduced pressure ($135^\circ\text{C}/0.06$ mmHg) with some decomposition or crystallized from a cold (-25°C) hexanes solution. Anal. Calcd for $\text{C}_{15}\text{H}_{39}\text{ClN}_6\text{Zr}$: C, 41.88; H, 9.14; N, 19.54. Found: C, 41.57; H, 8.97; N, 19.16. ^1H NMR (C_6D_6): δ 3.34 (sept, 3, 6.9 Hz, $\text{N}(\text{CH}(\text{CH}_3)_2)\text{N}(\text{CH}_3)_2$), 2.50 (s, 18, $\text{N}(\text{CH}(\text{CH}_3)_2)\text{N}(\text{CH}_3)_2$), 1.17 (d, 18, 6.9 Hz, $\text{N}(\text{CH}(\text{CH}_3)_2)\text{N}(\text{CH}_3)_2$). COSY NMR (C_7D_8): δ 47.73 (s, $\text{N}(\text{CH}(\text{CH}_3)_2)\text{N}(\text{CH}_3)_2$), 47.28 (s, $\text{N}(\text{CH}(\text{CH}_3)_2)\text{N}(\text{CH}_3)_2$), 26.45 (s, $\text{N}(\text{CH}(\text{CH}_3)_2)\text{N}(\text{CH}_3)_2$). IR (neat, KBr, cm^{-1}): 2958 vs, 2924 vs, 2860 vs, 2816 vs, 2771 s, 2740 s, 2709 w, 2650 vw, 2594 vs, 2472 vw, 2401 vw, 2221 vw, 2131 vw, 1971 vw, 1730 vw, 1595 s, 1454 vs, 1390 m, 1375 s, 1356 s, 1333 s, 1313 m, 1232 vs, 1167 vs, 1140 s, 1119 s, 1086 s, 1066 s, 1018 vs, 945 vs, 866 w, 852 m, 825 vw, 785 vs.

ZrCl(N(*t*-Bu)NMe₂)₃. This compound was synthesized and isolated as a yellow powder by using the method described for ZrCl(N(*i*-Pr)NMe₂)₃ (yield 0.198 g, 84%). ZrCl(N(*t*-Bu)NMe₂)₃ can be crystallized from a cold (-25°C) hexanes solution. Anal. Calcd for $\text{C}_{18}\text{H}_{45}\text{ClN}_6\text{Zr}$: C, 45.78; H, 9.60; N, 17.79. Found: C, 45.62; H, 9.46; N, 17.69. ^1H NMR (C_6D_6): δ 2.77 (s, 18, $\text{N}(\text{C}(\text{CH}_3)_3)\text{N}(\text{CH}_3)_2$), 1.29 (d, 27, $\text{N}(\text{C}(\text{CH}_3)_3)\text{N}(\text{CH}_3)_2$). $^{13}\text{C}\{^1\text{H}\}$ NMR (C_6D_6): δ 59.33 (s, $\text{N}(\text{C}(\text{CH}_3)_3)\text{N}(\text{CH}_3)_2$), 51.36 (s, $\text{N}(\text{C}(\text{CH}_3)_3)\text{N}(\text{CH}_3)_2$), 32.87 (s, $\text{N}(\text{C}(\text{CH}_3)_3)\text{N}(\text{CH}_3)_2$). IR (neat, NaCl, cm^{-1}): 2970 vs, 2956 vs, 2937 s, 2900 vs, 2872 s, 2818 s, 2785 m, 2767 s, 2729 vw, 2698 w, 1616 vw, 1603 vw, 1576 vw, 1558 vw, 1539 vw, 1506 vw, 1466 vs, 1383 s, 1356 vs, 1238 vs, 1201 vs, 1149 vs, 1085 w, 1068 w, 1036 s, 1016 vs, 943 vs, 872 w, 785 vs.

HfCl(N(*t*-Bu)NMe₂)₃. A procedure similar to the one used to prepare ZrCl(N(*t*-Bu)NMe₂)₃ produced HfCl(N(*t*-Bu)NMe₂)₃ as a yellow powder (yield 78%). Anal. Calcd for $\text{C}_{18}\text{H}_{45}\text{ClHfN}_6$: C, 38.64; H, 8.11; N, 15.02. Found: C, 38.51; H, 8.05; N, 15.07. ^1H NMR (C_6D_6): δ 2.79 (s, 18, $\text{N}(\text{C}(\text{CH}_3)_3)\text{N}(\text{CH}_3)_2$), 1.30 (d, 27, $\text{N}(\text{C}(\text{CH}_3)_3)\text{N}(\text{CH}_3)_2$). $^{13}\text{C}\{^1\text{H}\}$ NMR (C_6D_6): δ 59.44 (s, $\text{N}(\text{C}(\text{CH}_3)_3)\text{N}(\text{CH}_3)_2$), 51.36 (s, $\text{N}(\text{C}(\text{CH}_3)_3)\text{N}(\text{CH}_3)_2$), 33.06 (s, $\text{N}(\text{C}(\text{CH}_3)_3)\text{N}(\text{CH}_3)_2$). IR (neat, NaCl, cm^{-1}): 2960 vs, 2937 s, 2900 vs, 2872 vs, 2818 m, 1785 m, 2769 s, 2698 vw, 1558 vw, 1541 vw, 1523 vw, 1466 vs, 1441 s, 1385 s, 1354 vs, 1240 s, 1203 vs, 1153 s, 1086 m, 1038 s, 1016 vs, 945 vs, 901 w, 787 vs.

TaCl₃(N(*i*-Pr)NMe₂)₂. Lithium 1-*i*-propyl-2,2-dimethylhydrazide (0.362 g, 3.34 mmol) was added to a suspension of TaCl₅ (0.600 g, 1.67 mmol) in toluene (100 mL). The mixture was stirred at room temperature for 12 h and then filtered over Celite. The clear yellow filtrate was reduced in volume under vacuum (3 mL). Cooling the solution (-25°C) produced yellow crystals (yield 0.305 g, 38%). Anal. Calcd for $\text{C}_{10}\text{H}_{26}\text{Cl}_3\text{N}_4\text{Ta}$: C, 24.53; H, 5.35; N, 11.44. Found: C, 24.06; H, 5.16; N, 10.94. ^1H NMR (C_6D_6): δ 3.70 (sept, 2, 6.9 Hz, $\text{N}(\text{CH}(\text{CH}_3)_2)\text{N}(\text{CH}_3)_2$), 2.91 (s, 12, $\text{N}(\text{CH}(\text{CH}_3)_2)\text{N}(\text{CH}_3)_2$), 1.06 (d, 12, 6.9 Hz, $\text{N}(\text{CH}(\text{CH}_3)_2)\text{N}(\text{CH}_3)_2$). ^{13}C - ^1H COSY NMR (C_6D_6): δ 54.49 (s, $\text{N}(\text{CH}(\text{CH}_3)_2)\text{N}(\text{CH}_3)_2$), 48.86 (s, $\text{N}(\text{CH}(\text{CH}_3)_2)\text{N}(\text{CH}_3)_2$), 23.28 (s, $\text{N}(\text{CH}(\text{CH}_3)_2)\text{N}(\text{CH}_3)_2$). IR (Nujol, KBr, cm^{-1}): 2676 s, 2413 vw, 2303 vw, 1995 vs, 1723 vs, 1566 s, 1309 s, 1244 s, 1199 m, 1171 m, 1145 m, 1121 m, 1028 m, 1005 m, 963 m, 943 m, 890 m, 870 m, 777 s.

X-ray Crystallography. X-ray crystallographic data were collected for crystals of [LiN(*i*-Pr)NMe₂]₄ (colorless block), ZrCl(N(*i*-Pr)NMe₂)₃ (colorless block), ZrCl(N(*t*-Bu)NMe₂)₃ (colorless thick plate), and TaCl₃(N(*i*-Pr)NMe₂)₂ (colorless square column) grown from cold (-20°C) hexanes solutions and a crystal of [LiN(*t*-Bu)NMe₂·THF]₂ (colorless rectangular column) grown from a cold THF solution. Crystal data are presented in Table 1. All measurements were made with a Siemens SMART platform diffractometer equipped with a CCD area detector. The programs used in the X-ray crystallographic analyses were as follows: Data collection, Siemens SMART software (Siemens, 1996); cell refinement and data

Table 1. Crystal Data for [LiN(*i*-Pr)NMe₂]₄, [LiN(*t*-Bu)NMe₂·THF]₂, ZrCl(N(*i*-Pr)NMe₂)₃, ZrCl(N(*t*-Bu)NMe₂)₃, and TaCl₃(N(*i*-Pr)NMe₂)₂

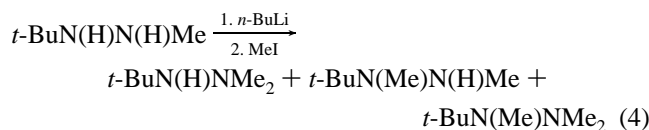
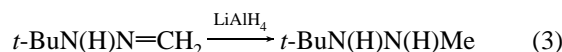
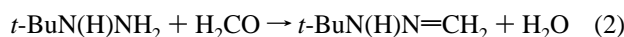
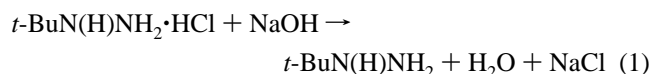
	[LiN(<i>i</i> -Pr)NMe ₂] ₄	[LiN(<i>t</i> -Bu)NMe ₂ ·THF] ₂	ZrCl(N(<i>i</i> -Pr)NMe ₂) ₃	ZrCl(N(<i>t</i> -Bu)NMe ₂) ₃	TaCl ₃ (N(<i>i</i> -Pr)NMe ₂) ₂
chem formula	C ₂₀ H ₅₂ N ₈ Li ₄	C ₂₀ H ₄₆ Li ₂ N ₄ O ₂	C ₁₅ H ₃₉ N ₆ ClZr	C ₁₈ H ₄₅ N ₆ ClZr	C ₁₀ H ₂₆ N ₄ Cl ₃ Ta
fw	432.46	388.49	430.19	472.27	489.65
cryst dimens, (mm ³)	0.45 × 0.45 × 0.35	0.35 × 0.30 × 0.15	0.35 × 0.35 × 0.15	0.25 × 0.20 × 0.15	0.40 × 0.10 × 0.10
space group	<i>P</i> 2 ₁ / <i>n</i> (monoclinic)	<i>P</i> 1 (triclinic)	<i>P</i> 1 (triclinic)	<i>Pbca</i> (orthorhombic)	<i>P</i> 2 ₁ / <i>n</i> (monoclinic)
<i>a</i> , Å	17.9907(11)	7.9754(11)	12.3737(7)	19.8844(12)	8.0886(5)
<i>b</i> , Å	9.3793(6)	8.8414(12)	13.4589(7)	16.1431(10)	13.6643(9)
<i>c</i> , Å	35.1404(22)	9.3659(13)	15.9761(9)	31.9630(19)	16.0468(10)
α, deg	90	78.889(2)	106.195(1)	90	90
β, deg	102.451(1)	77.113(2)	112.234(1)	90	92.374(1)
γ, deg	90	88.867(2)	91.632(1)	90	90
temp, °C	−50(2)	−50(2)	−50(2)	−50(2)	−50(2)
<i>Z</i>	8	1	4	16	4
<i>V</i> , Å ³	5790.1(6)	631.54(15)	2338.0(2)	10260.0(11)	1772.05(19)
<i>D</i> _{calcd} , g/cm ³	0.992	1.021	1.222	1.223	1.835
<i>μ</i> , mm ^{−1}	0.059	0.064	0.592	0.546	6.646
<i>R</i> , <i>R</i> _w ^a	0.0622, 0.1901 ^b	0.0420, 0.1122 ^c	0.0303, 0.0743 ^d	0.0331, 0.0674 ^e	0.0257, 0.0715 ^f

^a $R = \sum ||F_o| - |F_c|| / \sum |F_o|$; $R_w = [\sum w(F_o^2 - F_c^2)^2 / \sum w(F_o^2)^2]^{1/2}$. ^b $w = [\sigma^2(F_o^2) + (0.1096P)^2 + (5.7461P)]^{-1}$ where $P = (F_o^2 + 2F_c^2)/3$. ^c $w = [\sigma^2(F_o^2) + (0.0689P)^2 + (0.1526P)]^{-1}$. ^d $w = [\sigma^2(F_o^2) + (0.0433P)^2 + (1.5612P)]^{-1}$. ^e $w = [\sigma^2(F_o^2) + (0.0257P)^2 + (14.3376P)]^{-1}$. ^f $w = [\sigma^2(F_o^2) + (0.0584P)^2 + (0.7155P)]^{-1}$.

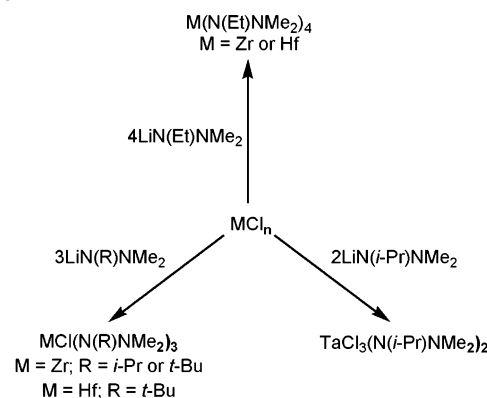
reduction, Bruker SAINT software (Bruker, 1999); and structure solution and refinement, SHELXL-97 (Sheldrick, 1997). The THF ligand in [LiN(*t*-Bu)NMe₂·THF]₂ was found to be severely disordered. Only the two major orientations were refined assuming 50% occupancies. Two of the isopropyl groups in ZrCl(N(*i*-Pr)NMe₂)₃ were found to be disordered approximately 65:35 over two slightly different orientations, and this was treated using ideal rigid body models based on one of the ordered groups.

Results and Discussion

Synthesis. The bulky hydrazine *t*-BuN(H)NMe₂ was synthesized from *t*-BuN(H)NH₂·HCl in 40% yield as the predominant component of a 90:5:5 mixture consisting of *t*-BuN(H)NMe₂, *t*-BuN(Me)N(H)Me, and *t*-BuN(Me)NMe₂, respectively. The sequence of reactions leading to the mixture containing *t*-BuN(H)NMe₂ consisted of neutralization of commercial *t*-BuN(H)NH₂·HCl with NaOH, reaction of *t*-BuN(H)NH₂ with formaldehyde to form the hydrazone *t*-BuN(H)N=CH₂,²¹ reduction of the hydrazone with LiAlH₄ to form the 1,2-dialkylhydrazine *t*-BuN(H)N(H)Me, and deprotonation of *t*-BuN(H)N(H)Me with *n*-BuLi followed by reaction with MeI (eqs 1–4). The hydrazine *t*-BuN(H)NMe₂ has only been observed previously in a mass spectrometry study.²² 1-Ethyl-2,2-dimethylhydrazine and 1-isopropyl-2,2-dimethylhydrazine and EtN(H)NMe₂ and *i*-PrN(H)NMe₂, were prepared similarly from H₂NNMe₂ via the hydrazone intermediates Me(H)C=NNMe₂ and Me₂C=NNMe₂, respectively, by following modified literature procedures.^{5,19,20}



Scheme 1



The ligand precursor LiN(*t*-Bu)NMe₂ was synthesized by reacting the mixture of *t*-BuN(H)NMe₂, *t*-BuN(Me)N(H)Me, *t*-BuN(Me)NMe₂ obtained in eq 4 with *n*-BuLi. The desired salt LiN(*t*-Bu)NMe₂ was separated from *t*-BuN(Me)NMe₂ and *t*-BuN(Me)N(Li)Me by distillation and fractional crystallization, respectively. The lithium salts of EtN(H)NMe₂ and *i*-PrN(H)NMe₂ were also prepared using *n*-BuLi. The LiN(R)NMe₂ salts for R = *i*-Pr and *t*-Bu are soluble in hexanes, benzene, and ether, while the salt for R = Et is soluble in ether and insoluble in hexanes and benzene.

A summary of the reactions leading to Zr, Hf, and Ta hydrazide complexes is presented in Scheme 1. Zirconium and hafnium tetrachloride reacted with 4 equiv of LiN(Et)NMe₂ to produce the homoleptic hydrazide complexes M(N(Et)NMe₂)₄ as waxy yellow solids in 50–60% yield after purification by sublimation. Reactions with the same stoichiometry involving LiN(R)NMe₂ for R = *i*-Pr and *t*-Bu yielded MCl(N(R)NMe₂)₃ (M = Zr, R = *i*-Pr or *t*-Bu; M = Hf, R = *t*-Bu) and unreacted LiN(R)NMe₂. By using the correct reaction stoichiometry, the MCl(N(R)NMe₂)₃ complexes were isolated as yellow powders in 80–90% yield. The zirconium derivative ZrCl(N(*i*-Pr)NMe₂)₃ sublimed under vacuum with some decomposition (135 °C/0.06 mmHg).

(21) Wang, S.-F.; Warkentin, J. *Can. J. Chem.* **1988**, *66*, 2256.

(22) Stolicová, M.; Kaszonyi, A.; Hronec, M.; Liptaj, T.; Stasko, A.; Lesko, J. *J. Mol. Cat. A* **2001**, *172*, 175.

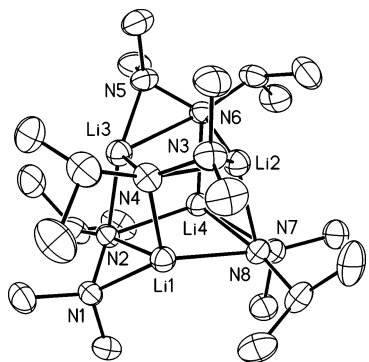


Figure 1. View of one of the two independent $[\text{LiN}(i\text{-Pr})\text{NMe}_2]_4$ units in the asymmetric unit showing the atom numbering scheme. Thermal ellipsoids are 40% equiprobability envelopes, with hydrogen atoms omitted.

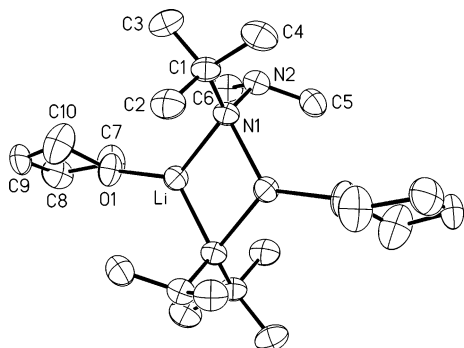


Figure 2. View of $[\text{LiN}(t\text{-Bu})\text{NMe}_2 \cdot \text{THF}]_2$ showing the atom numbering scheme. Only one orientation of the disordered THF ligand is shown. Thermal ellipsoids are 40% equiprobability envelopes, with hydrogen atoms omitted.

In an attempt to synthesize the homoleptic complex $\text{Zr}(\text{N}(i\text{-Pr})\text{NMe}_2)_4$, ZrCl_4 and 4 equiv of $\text{LiN}(i\text{-Pr})\text{NMe}_2$ were reacted in dioxane in a sealed pressure flask at $\sim 130^\circ\text{C}$. These forcing conditions produced a new product, which was thought to be $\text{Zr}(\text{N}(i\text{-Pr})\text{NMe}_2)_4$ by ^1H NMR analysis, but it could not be prepared without significant contamination by $\text{ZrCl}(\text{N}(i\text{-Pr})\text{NMe}_2)_3$.

Similar chemistry was observed using TaCl_5 . The reaction of 2 equiv of $\text{LiN}(i\text{-Pr})\text{NMe}_2$ with TaCl_5 produced yellow $\text{TaCl}_3(\text{N}(i\text{-Pr})\text{NMe}_2)_2$ after workup. Attempts to produce $\text{TaCl}_{5-x}(\text{N}(i\text{-Pr})\text{NMe}_2)_x$ complexes where $x > 2$ yielded $\text{TaCl}_3(\text{N}(i\text{-Pr})\text{NMe}_2)_2$ as the only isolable product, even when forcing conditions were employed (e.g., reactions in hexanes solvent in a sealed pressure flask at 60°C for 12 h). The trimethylhydrazide derivative $\text{TaCl}_3(\text{N}(\text{Me})\text{NMe}_2)_2$, prepared from $\text{MeN}(\text{SiMe}_3)\text{NMe}_2$ and TaCl_5 , has been reported.⁴

X-ray Structural Studies. The crystal structures of $[\text{LiN}(i\text{-Pr})\text{NMe}_2]_4$, $[\text{LiN}(t\text{-Bu})\text{NMe}_2 \cdot \text{THF}]_2$, $\text{ZrCl}(\text{N}(i\text{-Pr})\text{NMe}_2)_3$, $\text{ZrCl}(\text{N}(t\text{-Bu})\text{NMe}_2)_3$, and $\text{TaCl}_3(\text{N}(i\text{-Pr})\text{NMe}_2)_2$ (Figures 1–5, respectively) were determined. Selected bond lengths and angles are presented in Tables 2 and 3. The asymmetric units for $[\text{LiN}(i\text{-Pr})\text{NMe}_2]_4$, $\text{ZrCl}(\text{N}(i\text{-Pr})\text{NMe}_2)_3$, and $\text{ZrCl}(\text{N}(t\text{-Bu})\text{NMe}_2)_3$ consist of two similar independent molecules. Data for only one of the independent molecules are presented in the tables.

The four Li and four N_{amide} atoms of the tetramer $[\text{LiN}(i\text{-Pr})\text{NMe}_2]_4$ define a distorted cube with rhombus-shaped faces. Dimethylamine groups bridge four of the cube edges.

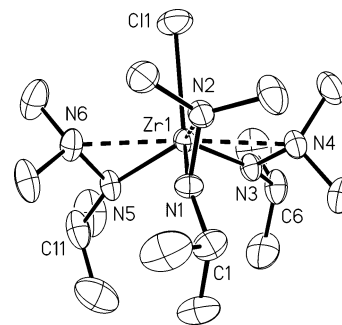


Figure 3. View of one of the two independent $\text{ZrCl}(\text{N}(i\text{-Pr})\text{NMe}_2)_3$ molecules in the asymmetric unit showing the atom numbering scheme. Thermal ellipsoids are 40% equiprobability envelopes, with hydrogen atoms omitted.

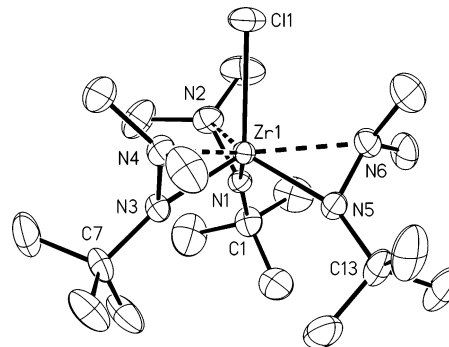


Figure 4. View of one of the two independent $\text{ZrCl}(\text{N}(t\text{-Bu})\text{NMe}_2)_3$ molecules in the asymmetric unit showing the atom numbering scheme. Thermal ellipsoids are 40% equiprobability envelopes, with hydrogen atoms omitted.

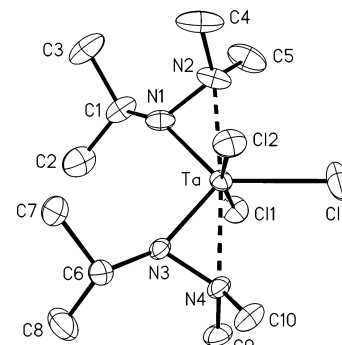


Figure 5. View of the $\text{TaCl}_3(\text{N}(i\text{-Pr})\text{NMe}_2)_2$ molecule showing the atom numbering scheme. Thermal ellipsoids are 40% equiprobability envelopes, with hydrogen atoms omitted.

The four-coordinate Li atoms in the cube are attached to three hydrazide N_{amide} atoms and one hydrazide N_{amine} atom. As emphasized in the ball-and-stick drawing I, the

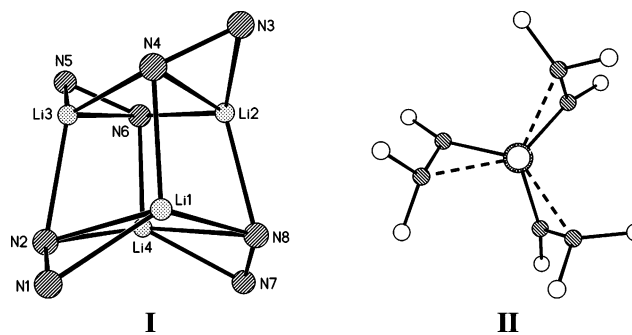


Table 2. Selected Bond Lengths (Å) and Angles (deg) for [LiN(*i*-Pr)NMe₂]₄ and [LiN(*t*-Bu)NMe₂·THF]₂

	[LiN(<i>i</i> -Pr)NMe ₂] ₄	[LiN(<i>t</i> -Bu)NMe ₂ ·THF] ₂
Li–N _{amide}	2.140(5), (2.082(5)–2.201(5)) ^a	2.024(3) (N _{amide} = N1) 2.040(3) (N _{amide} = N1')
Li–N _{amine}	2.004(5), (1.990(5)–2.022(5)) ^a	
Li–O1		1.966(3)
N _{amide} –N _{amine}	1.476(3), (1.475(3)–1.477(3)) ^a	1.4654(19)
N _{amide} –Li–N _{amide}	104.7(2), (103.2(2)–106.6(2)) ^a	105.94(13)
Li–N _{amide} –Li	72.9(2), (71.36(19)–73.61(18)) ^a	74.06(13)
Li–N _{amine} –N _{amide}	76.12(19), (75.48(18)–77.14(19)) ^a	
O1–Li–N1		126.78(16)
O1–Li–N1'		127.24(15)

^a Average value, (range of values).**Table 3.** Selected Bond Lengths (Å) and Angles (deg) for ZrCl(N(*i*-Pr)NMe₂)₃, ZrCl(N(*t*-Bu)NMe₂)₃, and TaCl₃(N(*i*-Pr)NMe₂)₂

	ZrCl(N(<i>i</i> -Pr)NMe ₂) ₃	ZrCl(N(<i>t</i> -Bu)NMe ₂) ₃	TaCl ₃ (N(<i>i</i> -Pr)NMe ₂) ₂
M–N1	2.084(3)	2.073(4)	1.958(4)
M–N2	2.320(3)	2.322(4)	2.217(4)
M–N3	2.051(3)	2.060(4)	1.938(3)
M–N4	2.340(3)	2.315(4)	2.223(3)
M–N5	2.063(3)	2.063(4)	
M–N6	2.339(3)	2.346(4)	
M–Cl	2.5098(10)	2.5308(14)	2.4345(10) (Cl = Cl1)
Ta–Cl2			2.4300(10)
Ta–Cl3			2.4220(12)
N1–M–N3	115.96(11)	102.44(15)	98.55(14)
N1–M–N5	103.63(11)	103.72(15)	
N1–M–Cl1	124.56(8)	117.05(11)	85.41(11)
N3–M–N5	96.72(11)	103.98(15)	
N3–M–Cl1	103.31(8)	115.34(11)	99.22(10)
N5–M–Cl1	109.09(9)	112.72(12)	
N2–M–Cl1	87.68(8)	83.20(12)	94.56(10)
N4–M–Cl1	95.41(8)	81.80(11)	86.71(9)
N6–M–Cl1	87.62(8)	83.32(11)	
M–N1–C1	153.1(2)	157.1(3)	145.4(3)
M–N1–N2	80.08(16)	80.7(2)	79.3(2)
M–N3–Cn	160.7(2) (<i>n</i> = 6)	157.5(3) (<i>n</i> = 7)	149.1(3) (<i>n</i> = 6)
M–N3–N4	82.01(16)	80.9(2)	80.97(19)
M–N5–Cn	160.3(3) (<i>n</i> = 11)	156.1(3) (<i>n</i> = 13)	
M–N5–N6	81.61(17)	82.0(2)	
C–N _{amide} –N _{amine}	116.9(3)–119.7(3)	121.6(3)–122.2(4)	120.5(3), 120.7(3)
N1–Ta–Cl2			101.28(11)
N1–Ta–Cl3			132.46(11)
N3–Ta–Cl1			99.22(10)
N3–Ta–Cl2			88.62(10)
N3–Ta–Cl3			128.91(10)
Cl1–Ta–Cl2			168.90(4)
Cl1–Ta–Cl3			84.43(4)
Cl2–Ta–Cl3			84.53(4)

[LiN_{amide}N_{amine}]₄ fragment has virtual *S*₄ symmetry. For the dimer [LiN(*t*-Bu)NMe₂·THF]₂, there is one molecule in the unit cell situated about an inversion center. The three-coordinate Li atom is bonded to oxygen of THF and two N_{amide} atoms of the hydrazides; thus, in contrast to the tetramer, the amine nitrogen of the hydrazide ligand in the dimer does not interact with Li. The idealized [LiN_{amide}]₂ core of [LiN(*t*-Bu)NMe₂·THF]₂ defines a rhombus with internal angles similar to those of the cube faces in [LiN(*i*-Pr)NMe₂]₄ (viz., in both molecules, N_{amide}–Li–N_{amide} ≈ 105° and Li–N_{amide}–Li ≈ 73°). One interesting feature of the tetramer is the longer Li–N_{amide} distances (av 2.140(5) Å) compared to the Li–N_{amine} distances (av 2.004(5) Å). An analogous difference was observed in [LiN(Et)N(H)Et]₆ (Li–N_{amide} = 2.121(3) Å and Li–N_{amine} = 2.020(3) Å), which has bridging N(H)Et groups.²³ In contrast, in [LiN(CH₂Ph)N-

(SiMe₃)CH₂Ph]₂, which has bridging N(SiMe₃)CH₂Ph groups, the Li–N_{amide} distance (av 1.939(8) Å) is shorter than the Li–N_{amine} distance (2.091(8) Å).²⁴ The salts [LiN(*i*-Pr)NMe₂]₄ and [LiN(*t*-Bu)NMe₂·THF]₂ appear to be the first structurally characterized examples of lithium trialkylhydrazides.

The structure of ZrCl(N(*i*-Pr)NMe₂)₃ closely resembles the structures of TiCl(N(Me)NMe₂)₃ and Ti(N(Me)NMe₂)₄.¹ In the latter Ti complex, the N_{amide} of an η¹-hydrazide ligand occupies the site of the Cl in the two chloride complexes. Like TiCl(N(Me)NMe₂)₃ and Ti(N(Me)NMe₂)₄, the idealized structure of ZrCl(N(*i*-Pr)NMe₂)₃ has *C*_s symmetry, with the mirror plane containing the atoms Zr, Cl, N1, and N2. In contrast to ZrCl(N(*i*-Pr)NMe₂)₃, the complex ZrCl(N(*t*-Bu)NMe₂)₃ has virtual *C*₃ symmetry with the three η²-hydrazide ligands coordinated to Zr in a propellerlike arrangement. A ball-and-stick drawing of ZrCl(N(*t*-Bu)NMe₂)₃ viewed down

(23) Nöth, H.; Sachdev, H.; Schmidt, M.; Schwenk, H. *Chem. Ber.* **1995**, *128*, 105.(24) Sachdev, H.; Preis, C. *Eur. J. Inorg. Chem.* **2002**, 1495.

the pseudo- C_3 axis (i.e., down the Cl–Zr bond) is shown in **II**. The overall geometry of $ZrCl(N(t\text{-Bu})NMe_2)_3$ is similar to the trimethylsilyl-substituted analog $ZrCl(N(SiMe_3)NMe_2)_3$, but in the latter case, the N_{amide} atoms rather than the N_{amine} atoms of the hydrazide ligands occupy the positions closest to the Cl (i.e., the NMe_2 groups in $ZrCl(N(SiMe_3)NMe_2)_3$ and $ZrCl(N(t\text{-Bu})NMe_2)_3$ are trans and cis, respectively, with respect to Cl).²⁵ In $ZrCl(N(t\text{-Bu})NMe_2)_3$, the $ZrCl(N_{amide})_3$ fragment of the structure defines a distorted tetrahedron with N–Zr–N angles of 102–104° and Cl–Zr–N angles of 113–117°.

The Zr– N_{amide} (2.051(3)–2.084(3) Å) and Zr– N_{amine} (2.315(4)–2.346(4) Å) distances in $ZrCl(N(i\text{-Pr})NMe_2)_3$ and $ZrCl(N(t\text{-Bu})NMe_2)_3$ are similar to those in eight-coordinate $Zr(N(Me)NMe_2)_4$ (Zr– N_{amide} = 2.0658(17) and 2.1127(19) Å; Zr– N_{amine} = 2.3063(19) and 2.4650(17) Å)¹ and in $ZrCl(N(SiMe_3)NMe_2)_3$ (av Zr– N_{amide} = 2.080(3) Å and av Zr– N_{amine} = 2.295(4) Å).²⁵ The Zr– N_{amide} distances in these hydrazide complexes fall close to or within the range of terminal Zr– N_{amide} distances (1.990(5)–2.108(3) Å) found in $[Zr(NMe_2)_2I(\mu\text{-}NMe_2)]_2$,²⁶ $Zr(NEt_2)_2Cl_2(THF)_2$, $Zr(NMe_2)_2Cl_2(THF)_2$,²⁷ $[Zr(NMe_2)_3(\mu\text{-}NMe_2)]_2$,²⁸ $(Me_2N)_2(THF)Zr(\mu\text{-}Cl)_2(\mu\text{-}NMe_2)Zr(NMe_2)_3$, $(Me_2N)_2(THF)Zr(\mu\text{-}Cl)_2(\mu\text{-}NMe_2)Zr(NMe_2)_2Cl$, and $(Me_2N)(THF)Cl_2Zr(\mu\text{-}Cl)_2Li(THF)_2$.²⁹ The Zr– N_{amine} distances in $ZrCl(N(i\text{-Pr})NMe_2)_3$ and $ZrCl(N(t\text{-Bu})NMe_2)_3$ are shorter than the Zr– N_{amine} distances in $ZrCl_3[N(SiMe_2CH_2NMe_2)_2]$ (2.447(4) and 2.437(4) Å) and $[CH_2CHNCH_2CH_2N(i\text{-Pr})CH_2CH_2N\text{-}i\text{-Pr}]Zr(CH_2Ph)_2$ (2.410–(5) Å),^{30,31} and therefore, the hydrazide ligands are best described as having η^2 coordination.

The $TaCl_3(N_{amide})_2$ fragment of $TaCl_3(N(i\text{-Pr})NMe_2)_2$ defines a distorted trigonal bipyramid in which the Cl1 and Cl2 atoms occupy the apical positions (Cl1–Ta–Cl2 = 168.90(4)°). The Ta– N_{amide} distances in $TaCl_3(N(i\text{-Pr})NMe_2)_2$ (1.938(3) and 1.958(4) Å) fall within the range of Ta– N_{amide} distances reported in the amide complexes $Ta(NR_2)_5$ (R = Me or Et), $Ta(\text{piperidinato})_5$, and $t\text{-Bu}Ta(NMe_2)_4$ (1.917(9)–2.238(9) Å),^{32–35} the cationic trimethylhydrazide complex $[Ta(N(Me)NMe_2)(S_2CNET_2)_3]^+$ (1.932(12) Å),⁴ and $Ta(N(t\text{-Bu})(NMe_2)_2(N(SiMe_3)NMe_2))$ (Ta–N($SiMe_3$) NMe_2 = 2.021–(7) Å; Ta– NMe_2 = 1.995(7) and 2.013(7) Å).²⁵ The Ta– N_{amine} distances in $TaCl_3(N(i\text{-Pr})NMe_2)_2$ (2.217(4) and 2.223(3) Å) are shorter than the comparable distances in Ta–

$(N\text{-}t\text{-Bu})(NMe_2)_2(N(SiMe_3)NMe_2)$ (2.350(7) Å)²⁵ and within experimental error of the one in $[Ta(N(Me)NMe_2)(S_2CNET_2)_3]^+$ (2.209(16) Å).⁴ The Ta– N_{amine} distances in $TaCl_3(N(i\text{-Pr})NMe_2)_2$ can also be compared, for example, to the Ta– N_{amine} distances in $Ta(N\text{-}2,6\text{-}i\text{-Pr}C_6H_3)X_3(\text{tmeda})$ (X = Cl, 2.325(7) Å; X = Br, 2.335(10) Å).³⁶ On the basis of the Ta– N_{amine} distance comparisons, it is reasonable to describe the hydrazide ligands in $TaCl_3(N(i\text{-Pr})NMe_2)_2$ as having η^2 coordination.

NMR Studies. The X-ray crystallographic studies indicate the $ZrCl(N(R)NMe_2)_3$ molecules have virtual C_s and C_3 symmetry in the solid state for R = *i*-Pr and *t*-Bu, respectively. As such, the ¹H NMR spectrum of $ZrCl(N(i\text{-Pr})NMe_2)_3$ should give rise to three doublets and three singlets of equal intensity if the structure is retained in solution. Similarly, the ¹H NMR spectrum of $ZrCl(N(t\text{-Bu})NMe_2)_3$ should show two *N*–*Me* singlets and a *t*-Bu singlet if the C_3 structure is static in solution. In fact, both molecules give simple room-temperature spectra, indicating fluxional processes are occurring that render the hydrazide ligands and their respective substituents equivalent. A low-temperature ¹H NMR spectrum of $ZrCl(N(i\text{-Pr})NMe_2)_3$ (–80 °C, toluene-*d*₈) was not significantly different from the room-temperature spectrum, suggesting the fluxional process was not slowed sufficiently to distinguish the resonances.

The tetramer $[LiN(i\text{-Pr})NMe_2]_4$ was shown to have virtual S_4 symmetry in the solid state. The expected ¹H NMR spectrum would consist of two methyl singlets (*NMe*) and two methyl doublets (*NCHMe*₂) of equal integrated intensity and a septet (*NCHMe*₂) with one-third relative intensity to the singlets and doublets. The room-temperature spectrum, however, had only a singlet, doublet, and septet, indicating fluxionality. A spectrum recorded for $[LiN(i\text{-Pr})NMe_2]_4$ at –80 °C in toluene-*d*₈ showed only broadening of the three resonances observed in the room-temperature spectrum, indicating the fluxionality persisted even at the low temperature.

Conclusion

The new, sterically encumbered hydrazine *t*-BuN(H)NMe₂ and its ligand precursor LiN(*t*-Bu)NMe₂ were synthesized. X-ray crystallographic analyses revealed a dimeric diamond-shaped structure for the THF adduct of LiN(*t*-Bu)NMe₂ and a tetrameric distorted-cube structure for the related salt LiN(*i*-Pr)NMe₂. The zirconium and hafnium complexes MCl(N(R)NMe₂)₃ (R = *i*-Pr, M = Zr; R = *t*-Bu, M = Zr or Hf) were synthesized from the LiN(R)NMe₂ salts and MCl₄ by metathesis reactions. By using less bulky ethyl-substituted hydrazide ligands, the homoleptic complexes M(N(Et)NMe₂)₄ (M = Zr or Hf) were prepared. Similar chemistry led to a tantalum complex having two hydrazide ligands, TaCl₃(N(*i*-Pr)NMe₂)₂. X-ray crystallographic studies on ZrCl(N(R)NMe₂)₃ (R = *i*-Pr or *t*-Bu) and TaCl₃(N(*i*-Pr)NMe₂)₂ revealed η^2 coordination for the hydrazide ligands.

Our interest in preparing these new hydrazide complexes was the possibility of using one or more of them as chemical

(25) Baunemann, A.; Kim, Y.; Winter, M.; Fischer, R. A. *Dalton Trans.* **2006**, 121.

(26) Lehn, J.-S. M.; Hoffman, D. M. *Inorg. Chem.* **2002**, *41*, 4063.

(27) Brenner, S.; Kempe, R.; Arndt, P. Z. *Anorg. Allg. Chem.* **1995**, *621*, 2021.

(28) Chisholm, M. H.; Hammond, C. E.; Huffman, J. C. *Polyhedron* **1988**, *7*, 2515.

(29) Wu, Z.; Diminnie, J. B.; Xue, Z. *Inorg. Chem.* **1998**, *37*, 2570.

(30) Fryzuk, M. D.; Hoffman, V.; Kickham, J. E.; Rettig, S. J.; Gambarotta, S. *Inorg. Chem.* **1997**, *36*, 3480.

(31) Giesbrecht, G. R.; Shafir, A.; Arnold, J. *Chem. Commun.* **2000**, 2135.

(32) Batsanov, A. S.; Churakov, A. I.; Howard, J. A. K.; Huges, A. K.; Johnson, A. L.; Kingsley, A. J.; Neretin, I. S.; Wade, K. *J. Chem. Soc. Dalton Trans.* **1999**, 3867.

(33) Davies, H. O.; Jones, A. C.; McKinnell, E. A.; Raftery, J.; Muryn, C. A.; Afzaal, M.; O'Brien, P. *J. Mater. Chem.* **2006**, *16*, 2226.

(34) Engering, J.; Peters, E.-M.; Jansen, M. Z. *Kristallogr.—New Cryst. Struct.* **2003**, *218*, 199.

(35) Chisholm, M. H.; Tan, L.-S.; Huffman, J. C. *J. Am. Chem. Soc.* **1982**, *104*, 4879.

(36) Heinselman, K. S.; Miskowski, V. M.; Geib, S. J.; Wang, L. C.; Hopkins, M. D. *Inorg. Chem.* **1997**, *36*, 5530.

vapor deposition precursors to metal oxide thin films.² Of the new complexes, only the homoleptic complexes $M(\text{N}(\text{Et})\text{NMe}_2)_4$ ($M = \text{Zr}$ or Hf) may be viable precursors because of the undesirable chlorine in the other compounds.

Acknowledgment. Dr. James Korp provided technical assistance with the crystal structure determinations. The Robert A. Welch Foundation supported this research.

Supporting Information Available: X-ray crystallographic data in CIF format for $[\text{LiN}(\textit{i}\text{-Pr})\text{NMe}_2]_4$, $[\text{LiN}(\textit{t}\text{-Bu})\text{NMe}_2 \cdot \text{THF}]_2$, $\text{ZrCl}(\text{N}(\textit{i}\text{-Pr})\text{NMe}_2)_3$, $\text{ZrCl}(\text{N}(\textit{t}\text{-Bu})\text{NMe}_2)_3$, and $\text{TaCl}_3(\text{N}(\textit{i}\text{-Pr})\text{NMe}_2)_2$. This material is available free of charge via the Internet at <http://pubs.acs.org>.

IC061483W